

STRUCTURAL PROPERTIES OF SUPERIONIC CONDUCTORS

Z. Vučić

Institute of Physics of the University of Zagreb
41 001 Zagreb Yugoslavia, POB 304, Bijenicka cesta 46

1. Introduction

Superionic conductors (solid electrolytes) are solid materials characterized primarily by their high ionic conductivities comparable with those found in liquid electrolytes (molten salts or aqueous solutions of salts). In general, SICs may be regarded as composed of two interpenetrating ionic subsystems: one is mobile, while the other builds a well defined solid form commonly named the cage. According to the type of the cage SICs fall into three categories: (i) inorganic crystalline solids, (ii) glasses, and (iii) polymers. The typical values of the ionic conductivity of the best superionic conductors are of the order of $1 (\Omega \text{ cm})^{-1}$. Among more than 300 SICs discovered so far, most of them belong to group (i), including both cation (H, Li, Na, K, Cu, Ag) and anion conductors (F, O, S).

A major factor motivating the investigation of SICs besides their interesting physical properties is their applicability in fuel cells, batteries, ion - selective membranes, gas sensors and other electrochemical devices. Although the task of fulfilling the most important technological demand - efficient energy storage - has not yet been fully accomplished, there are numerous other applications which have completely made up for the efforts invested in this field of research^{1, 2, 3}.

The most interesting and still unresolved problem of SICs is the origin of their high ionic conductivity. Within the model of noninteracting ions (particle density n) and in case of a one - dimensional periodic potential (height E) α ionic conductivity may be expressed by the following relation

$$\sigma = \frac{ng^2}{kT} \nu e^{-E/kT}$$

where q is the effective charge of an ion, l is the distance between potential minima, ν is the attempt frequency at which the particle approaches the potential barrier. There are also more complex formulas which involve correlation between particles⁵, but for our purposes this one is quite instructive.

It is obvious that the high ionic conductivity is associated with high particle density and low barrier height. Both these conditions are fulfilled in SICs. The above relation also shows how the ionic conductivity is related to the microscopic properties of the cage as well as to the entire structure of the SIC. The jump distance l is determined by the cage structure, and the attempt frequency ν is related to the particular vibrational modes of the mobile ions. The activation energy E consists of two terms: one is the barrier height between two crystallographic sites and the other is the configurational contribution originating from the arrangement of the surrounding mobile ions. Thus, the knowledge of the structure of ionic subsystem and its dynamics is extremely important for understanding the mechanisms of ionic transport in SICs. The present work is entirely devoted to the structure investigation of SICs, particularly of the diffuse X-ray scattering in nonstoichiometric cuprous selenide.

2. Diffuse x-ray scattering in superionic conductors

The first step towards the structure problem solution was made by Stroock⁶ in 1934. This work enabled the structural separation of two subsystems in AgI: the solid cage built of I^- ions, as a framework for the mobile Ag^+ ions, and the mobile ionic subsystem itself. The cage structure determination of any SIC never seemed to exceed the usually encountered problems. The cage crystallizes in one of the high symmetry lattices leaving a great number of empty crystal sites and open pathways between them available for the ion diffusion. On the contrary, the determination of the distribution of mobile ions within the cage has continuously been pointed out as a serious problem. What is the real distribution of mobile ions within the accessible space and what is the actual dynamical behaviour of ionic subsystem in time?

The answers to these questions would enable one to create a realistic model for calculation of the ionic conductivity. Among many specific techniques used to answer the posed questions we shall primarily concentrate upon the X-ray (and neutron) scattering techniques, which when applied to any SIC, reveal the strong diffuse scattering. It was shown that the diffuse scattering on SICs is at least ten times stronger than on normal ionic solids. This has not yet been quite satisfactorily explained.

In order to account for the enhanced diffuse X-ray scattering, the mobile ion subsystem has most often been treated as a quasiliquid^{8,9,10}, meaning that its contribution to the diffuse scattering is similar to that produced by amorphous solids or, more precisely, by binary solid solutions.

As long as only the powder samples were available, the quasiliquid model had no alternative. It was more or less successfully used for the interpretation of diffuse (as well as Bragg) X-ray scattering on many SICs like AgI, Ag₂Se, Ag₂S, AgCrS₂, CuI, CuBr etc. In the late 70's the first single crystal samples were prepared offering a specific diffuse scattering distribution in the reciprocal space which did not fit the quasiliquid approach at all. The new suggested model¹¹ asserted that the effect entirely stems from one-phonon X-ray scattering processes, thus excluding the possibility that diffuse scattering could contain any information about the average random distribution of mobile ions within the cage. It was the first attempt to treat the ionic subsystem as a correlated system.

The thermal origin of the diffuse X-ray scattering of an ordinary material (one phonon scattering) has been known for a long time¹². In SICs the same cause is assumed to be responsible for the enhanced diffuse X-ray scattering¹¹ since, using the neutron scattering technique, a very intense peak in phonon density of states has been measured at low frequencies ($\omega \approx \frac{1}{6} \omega_D$). It has been shown that this peak consists of dispersionless acoustic and optical modes¹³. Due to serious experimental problems the measurements were performed¹¹ only for β -AgI in its low temperature phase (at 160 K) for which the complete dispersion relations were determined. Using the

experimentally observed dispersion data, the diffuse one-phonon X-ray scattering intensity was calculated, showing excellent agreement with measured values. Unfortunately, neither the vibrational spectrum nor the diffusion scattering intensity calculations have been performed in the high conducting α phase of any SIC.

Most of the experimental work later on diminished significantly the quasiliquid approach reliability, clearly indicating that the mobile ions' behaviour is correlated rather than single-particle like. Besides the discovery of static ion correlated behaviour found in the one-dimensional hollandite¹⁴ and two-dimensional β -alumina¹⁵ recently several estimations of dynamic correlation in three-dimensional materials (Ag_2S ¹⁶, Ag_3SI ¹⁷, AgI ¹⁸) have been reported.

Our structural^{19,20} (as well as transport^{21,22,25} and thermal^{19,29,24}) properties investigations have been concentrated on the nonstoichiometric cuprous selenide which belongs to an almost isostructural group of copper and silver salts (AgI , Ag_2Se , Ag_2S , CuBr , Ag_2Te , Cu_2S , Cu_{2-c}Se , CuI , etc.). The deviation from stoichiometry in cuprous selenide leaves its structure unchanged, influencing only the average density of the copper ions. The ionic conductivity value is of order of $1 \Omega^{-1}\text{cm}^{-1}$ and decreases with increasing the deviation from stoichiometry^{22,25}. The cage unit cell is of $F\bar{4}3m$ symmetry²⁶ with 4 Se atoms in a and 4 Cu atoms in c positions. The rest of $4(1-c)$ Cu atoms are mobile occupying d and eventually b sites. Another structure with all copper atoms presumed to be mobile ($Fm\bar{3}m$ symmetry group) was also suggested²⁷.

Our main task has been to examine the temperature and composition dependence of the diffuse X-ray scattering of cuprous selenide in its high temperature α -phase where the high ionic conductivity is exhibited. To our knowledge such dependence has not yet been explored in detail for any SIC. We should also carefully observe the Bragg scattering behaviour, since the proper mobile ionic subsystem treatment is expected to make up for some obvious disagreement between the calculated and experimental Bragg scattering spectrum. As a matter of fact, a quite satisfying agreement between these two has been obtained

only for very few simple SIC systems, since the calculations have always been based on single ion treatment. For example, for the refinement of experimental data on the single crystal sample of α -AgI²⁸ the third and fourth-order thermal tensors had to be used.

In our case we chose to apply the dynamical correlated ion approach via the well defined phonon spectrum. The point is that well defined phonons may also exist in the mobile ion subsystem, which can be easily explained by assuming two distinguished types of behaviour for an ion in a certain crystallographic position. Most of the time an ion exhibits more or less harmonic vibrations around its crystal site. Occasionally, it jumps or diffuses to an adjacent or distant position where it resumes the oscillatory behaviour again. Along certain directions defined by the cage structure (the channels through the cage) the shallow potentials and consequently large ionic vibration amplitudes (compared to the other directions) are expected. In such a complex system one should expect two nearly independent types/modes of vibrations separated on energy scale: normal Debye modes at high frequencies related to the cage, and low energy modes related to the mobile ionic subsystem. These low energy modes are expected to be responsible for the remarkably intense diffuse X-ray scattering¹¹.

3. The one-phonon x-ray scattering: model calculations

The formalism describing the scattering of X-rays by phonons has been known since the time when the diffuse X-ray scattering was the only method available for the crystal elastic constants evaluation^{29,30}. The first step is to write down the dynamical structure factor (DSF) of the crystal in which ion displacements are correlated. The displacement correlation function treated within the harmonic approximation leads to the power series expansion^{29,30} in which the n^{th} term describes the contribution of the n -phonon scattering processes to the DSF. For $n = 0$ the static structure factor is obtained, while the term with $n = 1$ describes the scattering of an X-ray photon on a single phonon, etc. For the interpretation of the diffuse X-ray scattering we shall restrict to the $n = 1$ term. Taking well known

expression for the atomic displacement in the harmonic crystal and following the procedure given elsewhere³ the intensity of diffuse scattering is obtained.

$$I(\vec{Q}) = N \sum_{\vec{B}} \delta(\vec{Q} - (\vec{B} + \vec{q})) \sum_j |G_j(\vec{q}, \vec{Q})|^2 \frac{k_B T}{\omega^2(\vec{q})}$$

\vec{Q} is the diffraction vector, \vec{B} is the reciprocal lattice vector, \vec{q} is the phonon wave vector, ω is the phonon frequency and j is the polarization branch index. $G(\vec{q}, \vec{Q})$ is the structure factor of the cell for the diffuse scattering written as

$$G_j(\vec{q}, \vec{Q}) = \sum_{\vec{d}} e^{i\vec{Q}\vec{d}} f_d(Q) e^{-W_d(Q)} M_d^{-1/2} [\vec{Q} \cdot \vec{e}_j(\vec{q})]$$

where \vec{d} is the position of the atom within the cell, f_d is the atomic structure factor, W_d is the Debye-Waller factor, M_d is the atomic mass and \vec{e}_j is the phonon polarization vector.

Due to $\delta(\vec{Q} - (\vec{B} + \vec{q}))$ the diffuse X-ray scattering is spread out over the entire Brillouin zone, contrary to the Bragg scattering which is concentrated into a point. There are two distinct factors that determine the intensity distribution of diffuse scattering within the entire Brillouin zone: one remains the same for all Bragg points ($k_B T / \omega^2(\vec{q})$), while the other $|G(\vec{q}, \vec{Q})|^2$ changes from zone to zone in approximately the same way as the structure factor of the cell. The first one reveals that the diffuse scattering is the most intense for the lowest energy phonon branches. These are the weakly dispersive acoustic modes or low lying optical modes. In the following procedure we shall put to trial a model phonon spectrum consisting essentially of the acoustic modes. Thus, we may put $\omega_j(\vec{q}) = 2\pi v_{jq} |\vec{q}|$, where v_{jq} is the wave propagation velocity.

Another important part of the diffuse scattering structure factor $[\vec{Q} \cdot \vec{e}_j(\vec{q})]$ points out that the contribution to the diffuse scattering comes mainly from the phonons whose polarization vectors are collinear with the \vec{Q} vector. Therefore, the experimentally observed (on powder samples) strong diffuse scattering near the 220 Bragg peak, probably originates from the phonon having the polarization vector in or close to $\langle 110 \rangle$

direction (the cage channel directions).

From the previous discussion it is clear that the large amplitude, and consequently, low frequency³¹ ionic vibrations are restricted to the cage channels, that is the $\langle 110 \rangle$ directions (six of them, each with two possible orientations). Thus it is natural to choose the polarization vectors pointing in these directions. If two mutually perpendicular polarization vectors are chosen from the set $\langle 110 \rangle$, the third must be along one of the $\langle 100 \rangle$ directions in order to have the orthogonal basis. Having chosen one set of basis vectors, all other possible sets can be obtained using the point group symmetry ($\bar{4}3m$) operations.

Once the polarization vectors' directions are specified, all possible phonon wave vectors \vec{q} emerge quite naturally. There are 12 phonon wave vector directions of the type $\langle 110 \rangle$ and 6 of the type $\langle 100 \rangle$. In each specific direction, e. g. $[110]$, there is a number of phonons with wave vectors $\vec{q} = \pi\zeta/a \cdot [110]$, their magnitude ranging (almost continuously) from $q = 0$ to $q = \pi\sqrt{2}/a$. There is also a third group of phonons expected to contribute to the diffuse X-ray scattering which have only one polarization vector aligned with one of twelve $\langle 110 \rangle$ directions. The other two polarization vectors lie within the plane perpendicular to the first one. Corresponding phonon wave vectors fall into two subgroups: one with twelve phonon wave vector directions of the type $\langle 110 \rangle$, and the other filling continuously the cross section of the Brillouin zone and the plane perpendicular to the chosen $\langle 110 \rangle$ type polarization vector. Due to the large oscillation amplitudes in $\langle 110 \rangle$ directions, a much weaker dispersion than in any other direction, and accordingly, a low propagation velocity is expected for these polarization branches.

Taking into account the restriction to the acoustic phonons with the selected wave vectors we obtain the new diffuse X-ray scattering intensity expression

$$I(\vec{Q}) = \frac{Nk_B T}{16\pi^3} \sum_{i=1}^3 \sum_{\vec{B}} \delta(\vec{Q} - \vec{B} - \vec{q}_{p_i}) |D(\vec{Q})|^2 Q^2 \sum_j \frac{\cos^2 \alpha_j(\vec{q}_{p_i})}{v_{jq_p}^2 |\vec{q}_{p_i}|^2}$$

where p_i , $i = 1, 2, 3$ denote the listed groups of phonons characterized by their polarizations, $D(\vec{Q})$ is the mass normalized

structure factor of the cell, $\alpha_j(\vec{q}_{pi})$ is the angle between the \vec{Q} and $\vec{c}_j(\vec{q}_{pi})$ vectors and $V_{:q}$ is the propagation velocity along the tunnel direction.

In order to enable comparison with the experiments performed on the powder samples, the last expression has to be integrated over all directions of \vec{Q} , keeping its magnitude constant. The integration is limited to the parts of surface of the sphere of radius Q within the Brillouin zones centered at the Bragg points \vec{B} (having the same $|\vec{B}|$) for all phonon wave vectors \vec{q}_{pi} which fulfil the condition $\vec{Q} = \vec{B} + \vec{q}_{pi}$.

After some cumbersome calculation, the total diffuse X-ray scattering intensity, now depending only on the magnitude of the diffraction vector $|\vec{Q}|$ may be formally written as

$$I(Q) = \frac{Nk_B T}{16\pi^3 V_{110}^2} |D(Q, B)|^2 Q^2 M(B) \sum_{i=1}^3 Z_{pi}(Q, B)$$

where $M(B)$ is the multiplicity of the Bragg point $|\vec{B}|$, and $Z_{pi}(Q)$ are three different complicated expressions⁹² giving a detailed account of contributions of the three groups of phonons described earlier.

4. Results and discussion

The experimentally obtained intensity data should be corrected in the usual manner¹² in order to extract the contribution corresponding to one-phonon X-ray scattering. After that we are left with six unknown quantities to be determined during the fitting procedure: the background scattering (I_B), scaling constant k , three Debye - Waller factors W_{Se}^{cage} , W_{Cu}^{cage} , W_{Cu}^{mobile} and the renormalized wave propagation velocity. The first two of them can be obtained independently, from the least squares fit of the experimental data in the curve tail at high Q values, where all other contributions to the diffuse scattering are negligible compared to the background scattering and the total Compton scattering. Having determined I_B and k from the successful fitting procedure (shown in Fig. 2.a), we are still to determine the values of four unknowns. This number can be further reduced, bearing in mind that the Debye - Waller factors are calculated within the described phonon

spectrum^{2p}. As we are dealing with two distinct weakly bound subsystems, only two qualitatively different DW factors are expected. Thus

$$W_{\text{Se}}^{\text{cage}} = \frac{1}{2 M_{\text{Se}}} b T Q^2; \quad W_{\text{Cu}}^{\text{cage}} = \frac{1}{2 M_{\text{Cu}}} b T Q^2; \quad W_{\text{Cu}}^{\text{mob}} = \frac{1}{2 M_{\text{Cu}}} b_M T Q^2$$

where b and b_M represent the full but slightly renormalized vibrational spectrum of the cage and the mobile ionic subsystem^{2p}, respectively. Remaining three unknown parameters were determined using least squares fit through the experimental data sets. The experimental data together with the values obtained from the fit are shown in Fig. 1.

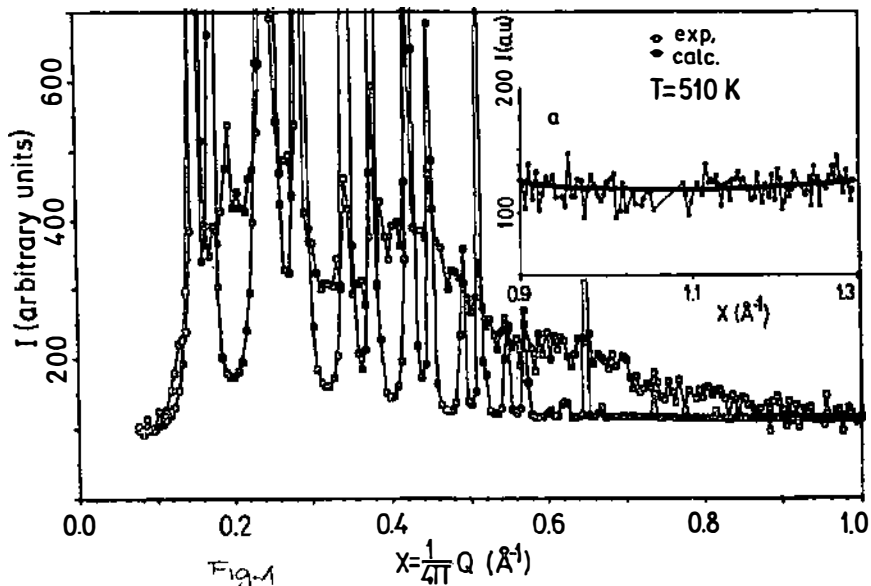


Fig.1 Intensity (I) of diffuse scattering vs. diffraction wave vector $Q/4\pi$ for the sample $\text{Cu}_{1.8}\text{Se}$ at 510 K, experimental (open symbols) and calculated (full symbols) data. The calculated data have been obtained assuming x-ray scattering on low energy acoustic phonon modes within the normal Debye phonon spectrum. Insert a) Least squares fit (full line) through the tail of the measured intensity curve.

The agreement is obviously poor. After a brief analysis of

different parameters influence it becomes obvious that the main cause of disagreement are the divergences near each $Q = B$, originating from the expression

$$I \propto 1/q^2$$

This means that for our purposes the acoustic phonon concept is at least not a decisive one. The intensity divergences near each B are the consequence of the starting definition of the single ion displacement. Within the harmonic crystal approximation, the position of any ion at time t is a linear function of the positions and momenta of all ions in the crystal at time zero.

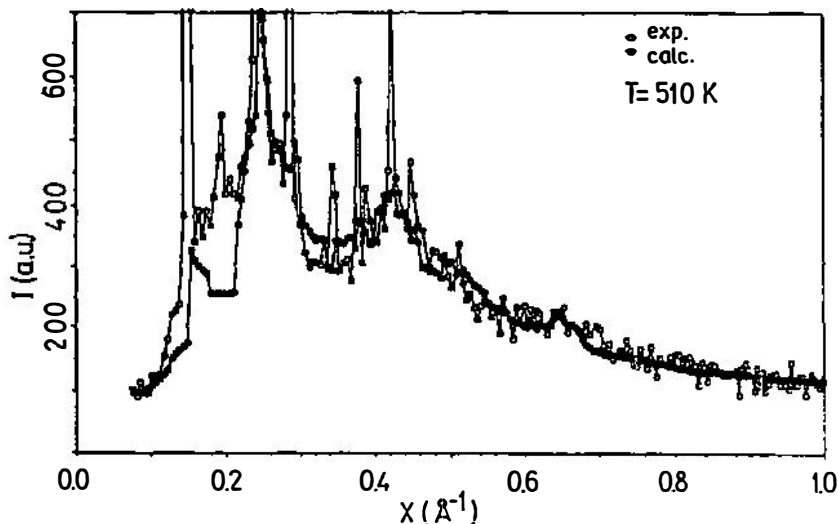


Fig. 2 Intensity (I) of diffuse x-ray scattering vs. diffraction wave vector $Q/4\pi$ for the sample $\text{Cu}_{1.8}\text{Se}$ at 510 K, experimental (open symbols) and calculated (full symbols) data. The calculated data have been obtained assuming x-ray scattering on low energy almost dispersionless optical phonon modes related to ion-cluster vibrations.

Due to the evident lack of long range order in the ionic subsystem and to its high mobility, we should rather consider ion - displacement correlations of limited spatial, and perhaps

also of limited temporal range.

So, instead, we introduce a displacement of an ion that is determined by its limited - size neighbourhood. As a consequence, the correlation function of the ion displacements can be calculated using the convenient and well - known Ornstein - Zernike approximation³¹. After the Fourier transformation³¹ we get the reciprocal space intensity distribution, with the divergences near each B removed.

$$I \propto 1 / \left(\frac{1}{\xi^2} + q^2 \right)$$

where ξ is the correlation length of the ionic subsystem.

Applying the least squares fit program once again, this time with four fitting parameters (including ξ) we get the agreement between the experimental and calculated values enormously improved (Fig. 2.). It should also be noted that the model gives a very good account of the temperature dependence, too³².

Introducing the correlation length as the fitting parameter had no influence on the b and b_M values. They are $b = 0.21 \times 10^{-2}$ and $b_M = 0.85 \times 10^{-2}$ corresponding to mean Cu atom displacements of 0.13 Å and 0.26 Å, respectively. These values fall within the range expected from the comparison with the results³³ for other SICs.

The most interesting parameter, the correlation length ξ is found to be 15 ± 5 Å, which is about four times the interionic distance along the channel direction. This value, being temperature independent in the whole temperature range (300 - 510 K), is the same as the short range correlation length found in one-dimensional hollandite¹⁴, two-dimensional Na- β -alumina¹⁵ and recently in three-dimensional Ag_2S ¹⁶.

Thus, we may say that there are strong indications of the existence of short-range ordered ionic clusters which, irrespective of their life-time, are responsible for the observed diffuse scattering. Two contributions are then expected. The first, described within the presented model, is a dominant one (80 - 90%) stemming exclusively from dynamics of clusters (optical phonons). The second one, covering the rest of the observed diffuse scattering, stems from the short-range ordering

of ions within the cluster. The latter contribution may be observed separately if one measures the diffuse scattering of a single crystal along certain directions. Indeed, the preliminary measurements of diffuse scattering on single crystals^{9,2} show the series of weak and wide Lorentzian shaped peaks in reciprocal space slightly ($\approx 2\%$) incommensurate with the cage lattice. Their existence, distribution in reciprocal space and their widths indicate the short range ordered ionic lattice superstructure with doubled (and fourfolded) incommensurate periodicity. It gives rise to the diffuse scattering, which, when transformed to the powder response just fits the difference between the model and experimental data .

Do we now understand the problems of ionic conductivity better? In a certain sense, yes, since we now know the attempt frequency and the correlation length needed for the configurational part of activation energy calculation. In order to calculate it more exactly, we need further informations about statics and dynamics of the short range correlation of ionic subsystem.

I am extremely grateful for permanent help of O. Milat and for the assistance of J. Gladić, M. Ilić and V. Horvatić at various stages of preparing the article.

1. R. A. Huggins, *Solid State Ionics*, 5 (1981) 15.
2. W. van Gool (ed.), *Fast Ion Transport in Solids - Solid State Batteries and Devices*, North - Holland, Amsterdam - London 1973.
3. W. Weppner and H. Schulz (eds.), *6th Int. Meeting on Solid State Ionics*, Garmisch - Partenkirchen, FRG, 6 - 11 Sept. 1987., *Solid State Ionics*
4. H. Sato, R. Kikuchi in G. D. Mahan, W. L. Roth (eds.), *Superionic Conductors*, Plenum Press, New York and London 1976., p. 135.
5. D. P. Almond and A. R. West, *Nature* 306 (1983) 456.
6. L. W. Strock., *Z. Phys. Chem.* B25 (1934) 441.
7. S. Hoshino, *J. Phys. Soc. Japan* 12 (4) (1957) 315.
8. J. Schreuers, M. H. Mueller, L. H. Schwartz, *Acta Cryst.* A32 (1976) 618.
9. T. Sakuma, K. Iida, K. Honma, H. Okazaki, *J. Phys. Soc. Japan* 43 (2) (1977) 538.

10. Y. Tsuchiya, *J. Phys C* 14 (1981) 1409.
11. H. U. Beyeler, P. Brüesch, T. Hibma, W. Bührer, *Phys. Rev. B* 18 (9) (1978) 4570.
12. R. W. James, *Optical Principles of the Diffraction of X - rays*, G. Bell & Sons, London 1948.
13. W. Bührer, R. M. Nicklow, P. Brüesch, *Phys. Rev. B* 17 (8) (1978) 3362.
14. H. U. Beyeler, *Phys. Rev. Lett.* 37 (1976) 1557.
15. Y. Le Cars, R. Comes, L. Deschamps and J. Therry, *Acta Cryst.* A30 (1974) 305.
16. B. H. Grier, S. M. Shapiro, R. J. Cava, *Phys. Rev. B* 29 (7) (1984) 3810.
17. K. Shibata, S. Hoshino, *J. Phys. Soc. Japan*, 54 (10) (1985) 3671.
18. R. J. Cava, R. M. Fleming, E. A. Rietman, *Solid State Ionics* 9 & 10 (1983) 1347.
19. Z. Vučić, O. Milat, V. Horvatić, Z. Ogorelec, *Phys. Rev B* 24 (1981) 5398.
20. O. Milat, Z. Vučić, B. Ružić, *Solid State Ionics* 23 (1987) 37.
21. Z. Vučić, V. Horvatić, Z. Ogorelec, *J. Phys. C* 15 (1982) 3539.
22. M. Horvatić, Z. Vučić, *Solid State Ionics* 13 (1984) 117.
23. M. Horvatić, Z. Vučić, J. Gladić, M. Ilić, I. Aviani, *Solid State Ionics* 27 (1988) 31.
24. I. Aviani, Z. Vučić, M. Horvatić, J. Gladić, *Solid State Comm.* 64 (1987) 1317.
25. M. Horvatić, I. Aviani, M. Ilić, *Solid State Ionics* 34 (1989) 21.
26. W. Borchert, *Z. Kristallogr.* 106 (1945) 5.
27. R. M. Murray, R. D. Heyding, *Can. J. Chem.* 53 (1975) 878.
28. R. J. Cava, F. Reidinger, B. J. Wuensch, *Solid State Comm.* 24 (1977) 411.
29. N. W. Ashcroft, N. D. Mermin, *Solid State Physics*, Saunders College, Philadelphia 1976.
30. S. W Lovesey in S. W. Lovesey and T. Springer (eds.), *Dynamics of Solids and Liquids by Neutron Scattering*, Springer - Verlag, New York 1977.
31. B. Dorner and R. Comes in *ibid.*
32. Z. Vučić, *Thesis, unpublished*
33. A. F. Wright, B. E. F. Fender, *J. Phys. C* 10 (1977) 2261.